Fizika Nizkikh Temperatur, 2006, v. 32, Nos. 4/5, p. 483–498

Theory of antiferromagnetic pairing in cuprate superconductors

(Review article)

N.M. Plakida

Joint Institute for Nuclear Research, 141980 Dubna, Russia
E-mail: plakida@htsun1.jinr.ru

Received September 15, 2005

A review of the antiferromagnetic exchange and spin-fluctuation pairing theory in the cuprate superconductors is given. We briefly discuss a phenomenological approach and a theory in the limit of weak Coulomb correlations. A microscopic theory in the strong correlation limit is presented in more detail. In particular, results of our recently developed theory for the effective p–d Hubbard model and the reduced t–J model are given. We have proved that retardation effects for the antiferromagnetic exchange interaction are unimportant that results in pairing of all charge carriers in the conduction band and high T_c proportional to the Fermi energy. The spin-fluctuation interaction caused by kinematic interaction gives an additional contribution to the d-wave pairing. Dependence of T_c on the hole concentration and the lattice constant (or pressure) and an oxygen isotope shift are discussed.

PACS: **74.20.–z**, 74.20.Mn, **74.72.–h**

Keywords: high-temperature superconductivity, strong electron correlations, Hubbard model, antiferromagnetic exchange interaction, spin-fluctuations.

1. Introduction

Twenty years have passed since the discovery of the high-temperature superconductivity (HTSC) in cuprates by Bednorz and Müller [1]. While extensive experimental investigations over the years have produced a wealth of high-precision data resulting in a consistent description of the major physical properties of the cuprate superconductors, the pairing mechanism of HTSC is still under hot debate. To answer the question of only the cuprate superconductors demonstrate $T_c > 100$ K, one should look for particular properties of these compounds which single them out among other materials. A unique property of cuprates is that they belong to charge-transfer insulators with a small splitting energy between $3d$ copper and $2p$ oxygen levels and large Coulomb correlations at $3d$ copper states [2]. This peculiar electronic structure of cuprates results in a huge antiferromagnetic (AFM) superexchange interaction of the order of $J \simeq 1500$ K which brings about a long-range AFM order in the parent insulator compounds and ensures strong short-range AFM dynamical spin fluctuations in metallic and superconducting states (see, e.g., [3]). Recent angle-resolved photoemission spectroscopy (ARPES) studies proved an important role of AFM spin fluctuations in the electron dispersion renormalization close to the Fermi surface (the «kink» phenomenon — see, e.g., [4]). Therefore, one can suggest that strong interaction of charge carriers in cuprates with AFM spin fluctuations is responsible for their anomalous normal state properties and can be an origin of the superconducting pairing as proposed by Anderson [5].

At the first International Conference on High-Temperature Superconductors and Materials and Mechanisms of Superconductivity (Interlaken, Switzerland 1988), Robert Schrieffer in his final remarks said that «a horse race has started» in search of a mechanism of the high-temperature superconductivity and said that he stakes «on the antiferromagnetic horse». The author believes that Robert Schrieffer has won the race. Below we give a brief review of the magnetic mechanism of the high-temperature superconductivity

in cuprates based on the antiferromagnetic exchange and spin-fluctuation pairing theory (for detail see [6]).

1.1. Phenomenological approach

Earlier the magnetic pairing mechanism was proposed for systems with heavy fermions [7–9] where the *d*-wave pairing was observed. Later on it was suggested that this mechanism could be responsible for the high-temperature superconductivity [10]. It was shown that, under the exchange of AFM paramagnons, an attraction appears in the *d*-channel and acts most effectively near the AFM instability [11,12]. The spin-fluctuation pairing mechanism on the basis of phenomenological approach was considered by several groups (see, e.g., [13–25]).

For the AFM ground state, transverse fluctuations of the AFM order parameter ensure an effective attraction which is favorable for a magnetic pairing mechanism. To describe the pairing in the AFM state, a concept of the «*spin bag*» was developed by Schrieffer et al. [13]. This approach was based on the assumption of a local depression by a hole of the AFM gap in the electron spectrum. As a result, a magnetic polaron — a spin bag, which moves together with the cloud of spin deformation, appears. In this case, two holes, i.e., polarons, attract each other due to the overlap of their regions of deformation of the AFM order. An extended analysis has shown that the longitudinal spin fluctuations lead to a singlet pairing with the maximum contribution coming from the *d*-wave channel. Although in the copper-oxide compounds superconductivity arises for hole concentration $n_h \geq 0.05$, where long-range AFM order is already destroyed, due to the small superconducting correlation length ξ_0 the theory can be applied in the region $\xi_N > \xi_0$ (where ξ_N is an AFM correlation length).

In the paramagnetic phase, the contribution of spin fluctuations near the AFM wave vector $\mathbf{Q}_{AF} = (\pi, \pi)$ leads to the appearance of a pseudogap in the electron spectrum near half-filling [14]. The additional exchange of the AFM spin fluctuations for two quasiparticles (QPs), the «spin bags», decreases their energy, similar to the case of the long-range AFM order, and results in their mutual attraction. In this case, an effective interaction potential $V(\mathbf{k},\mathbf{k}')$ is attractive in the range of a small momentum transfer $\mathbf{q} = \mathbf{k} - \mathbf{k}'$ and is of a repulsive character for large $\mathbf{q} \simeq \mathbf{Q}_{AF}$. Therefore, in this case, the symmetry of the superconducting order parameter, $\Delta(\mathbf{k})$, and the value of T_c strongly depend on the form of the Fermi surface for QPs. These calculations were performed under an assumption of weak or intermediate Coulomb correlations and in the framework of the one-band Hubbard model (for $U \leq 4t$). A generalization of the theory for the case of strong correlations and for the multi-band *p–d* model is important to compare its conclusions with experiments in the copper-oxide superconductors.

Interaction between QPs on a two-dimensional square lattice under an exchange of AFM paramagnons was most extensively studied by Pines et al. [16–21]. They have considered a model of a nearly antiferromagnetic Fermi liquid (NAFL) where interaction between two QPs with spins $\boldsymbol{\sigma}_1$, $\boldsymbol{\sigma}_2$ is mediated by an exchange of spin fluctuations [19]

$$V_{\text{mag}}^{\text{eff}}(\mathbf{q},\omega) = g^2 \chi(\mathbf{q},\omega)\, \boldsymbol{\sigma}_1 \cdot \boldsymbol{\sigma}_2 \,. \qquad (1)$$

The dynamical spin susceptibility was described by a phenomenological model

$$\chi_{MMP}(\mathbf{q},\omega) = \frac{\alpha \xi^2}{1 + \xi^2 (\mathbf{Q}_{AF} - \mathbf{q})^2 - i\omega / \omega_{sf}} \,, \qquad (2)$$

where $\xi(T)$ is the AFM correlation length and $\hbar\omega_{sf}$ is the typical energy of AFM fluctuation. The spin susceptibility (2) at large values of $\xi(T)$ can reach high values at the AFM wave vector $\mathbf{q} = \mathbf{Q}_{AF}$. The authors numerically solved the Eliashberg equations in $(\mathbf{q},\omega)$-space and observed superconductivity in the *d*-wave channel [20] with $T_c \sim 90$ K for a comparatively modest value of coupling constant g. Studies of the temperature dependence of the superconducting gap $\Delta(T)$ have shown that near T_c the gap grows rapidly when the temperature decreases and reaches a maximum value $2\Delta(0)/kT_c = 6–8$ which agrees with experiments. In these calculations, the high T_c and the *d*-wave pairing are conditioned by a strongly anisotropic interaction due to the AFM spin fluctuations. Strong enhancement of the spin susceptibility (2) near AFM wave vector $\mathbf{Q}_{AF}$ is capable of bringing about high T_c in spite of strong pair-braking effects due to spin scattering. Studies of normal state properties of the cuprate superconductors have supported the NAFL model. Therefore, the authors have concluded that the mechanism for high T_c is electronic and magnetic in origin. However, several critical remarks concerning the NAFL model should be mentioned [26,27].

1.2. Microscopic theory

As was pointed out by Anderson [27], in conventional metals only ferromagnetic electron correlations can occur, while AFM interaction in the copper oxides is of superexchange origin. The latter can be properly described only in the framework of models with strong electron correlations like the Hubbard model or

the t–J model [5]. The one-band Hubbard model reads [28]:

$$H = -t\sum_{\langle ij\rangle\sigma}(a^{+}_{i\sigma}a_{j\sigma} + \text{h.c.}) + U\sum_{i} n_{i\uparrow}n_{i\downarrow}, \quad (3)$$

where the first term is the kinetic energy of electrons with an effective transfer integral t for a pair of nearest neighbor sites, $\langle ij\rangle$, $i > j$, and U is a Coulomb single-site energy. For a large enough $U > U_c \simeq W$ (W is the band width for free electrons, $W = 8t$ for a two-dimensional square lattice) the model (3) describes the Hubbard – Mott insulator at half-filling, $n = 1$. In the strong correlation limit, $U >> t$, when only singly occupied sites are taken into account since a doubly occupied site costs a large additional energy U, the model (3) can be reduced to the t–J model [27]:

$$H_{t-J} = -t\sum_{\langle ij\rangle,\sigma}(\tilde{a}^{+}_{i\sigma}\tilde{a}^{+}_{j\sigma} + \text{h.c.}) + J\sum_{\langle ij\rangle}(\mathbf{S}_i\mathbf{S}_j - \frac{1}{4}n_i n_j). \quad (4)$$

Here the projected electron operators $\tilde{a}^{+}_{i\sigma} = a^{+}_{i\sigma}(1 - n_{i-\sigma})$ act in a subspace without double occupancy and $n_i = \sum_{\sigma}\tilde{a}^{+}_{i\sigma}\tilde{a}_{i\sigma}$ is the number operator for electrons. The second contribution, written in terms of the spin operators $S^{\alpha}_{i} = (1/2)\sum_{s,s'}\tilde{a}^{+}_{is}\sigma^{\alpha}_{s,s'}\tilde{a}_{is'}$, describes an AFM exchange interaction with the energy $J = 4t^2/U$ for electrons on nearest neighbor sites.

So starting from the original Hubbard model (3) for conventional fermions with the Coulomb repulsion U we have arrived to the t–J model (4) for fermion-like particles projected onto the singly occupied Hubbard subband which obey the nonfermionic commutation relations with an additional AFM exchange interaction between them. It should be pointed out that the exchange interaction between these «projected» fermions results from the so-called kinematic interaction caused by the nonfermionic commutation relations. The latter present great obstacles for employing the conventional diagram technique for fermions. Presently there are no rigorous methods to study models with strong electron correlations like (3) or (4) for dimensions $D \geq 2$. The recently developed dynamical mean-field theory (for a review see [29,30]) which is exact in the infinite dimensions is unable to treat nonlocal correlations as, e.g., the exchange interaction, and to study the nonlocal d-wave type superconducting pairing. To overcome this deficiency a dynamical cluster theory was elaborated (for a review see [31]). In this connection we should mention the studies of superconducting pairing within the dynamical cluster approximation in [32,33].

1.2.1. Weak correlation limit

In the weak correlation limit, $U << t$, a perturbation approach for the Hubbard model (3) can be applied. In a number of studies (see [34–37] and references therein) a self-consistent set of equations in the fluctuation-exchange approximation (FLEX) [38] for the single-electron Green functions and the spin and charge susceptibility were numerically solved. The FLEX approximation was also applied for the three-band p–d model with Coulomb repulsion U on copper sites [39] and for electronically doped cuprates [40]. Within this approach a qualitative description of the copper-oxide materials was obtained at moderate and large doping regimes at intermediate values of the Coulomb repulsion, $U \leq W/2 = 4t$. However, starting from the Fermi-liquid picture, the theory fails to describe the underdoped regime with strong correlations and large values of the Coulomb repulsion, $U \geq W$, close to the insulating (and AFM) state. In that region higher order corrections to the effective interactions mediated by spin fluctuations are important [26].

Let us briefly discuss these studies of the strong coupling equations for the Hubbard model in the weak correlation limit [34–37]. In the framework of FLEX, a self-consistent system of equations for the diagonal $G(p,\omega_n)$ and the off-diagonal $F(p,\omega_n)$ single-electron Green functions was written as (see, e.g., [35]):

$$G(p,\omega_n) = \frac{i\omega_n Z(p,\omega_n) + X(p,\omega_n)}{[i\omega_n Z(p,\omega_n)]^2 - X^2(p,\omega_n) - \varphi^2(p,\omega_n)}, \quad (5)$$

$$F(p,\omega_n) = \frac{\varphi(p,\omega_n)}{[i\omega_n Z(p,\omega_n)]^2 - X^2(p,\omega_n) - \varphi^2(p,\omega_n)}, \quad (6)$$

with $X(p,\omega_n) = \epsilon_p - \mu + \xi(p,\omega_n)$. Here we used the standard notation for the renormalization parameter $Z(p,\omega_n)$, the energy shift $\xi(p,\omega_n)$, and the gap parameter $\varphi(p,\omega_n)$ in the Eliashberg-type equations for the Nambu frequency $\omega_n = \pi T(2n+1)$ and the 2D wave vector $p = (p_x, p_y)$. The interactions are mediated by the spin $V_s(q,\omega_n)$ and the charge $V_c(q,\omega_n)$ fluctuations calculated in the random phase approximation (RPA). The irreducible spin $\chi^{s}_{0}(q,\omega_n)$ and charge $\chi^{c}_{0}(q,\omega_n)$ susceptibility in the RPA formulas are defined self-consistently in a one-loop approximation by using the Green functions (5), (6):

$$\chi^{s,c}_{0}(q,\omega_n) = -T\sum_{k,m}[G(k+q,\omega_n+\omega_m)G(k,\omega_m) \pm$$

$$\pm F(k+q,\omega_n+\omega_m)F(k,\omega_m)],$$

where +(−) stands for $\chi_0^s(\chi_0^c)$. Numerical solutions of the self-consistent set of equations for intermediate values of the Coulomb repulsion, $U \le 4t$, for the full momentum- and frequency-dependent renormalization parameter $Z(p,\omega)$, the energy shift $\xi(p,\omega)$, and the gap function $\Delta(p,\omega) = \varphi(p,\omega)/Z(p,\omega)$ have been obtained. The gap function has been found to have the $d_{x^2-y^2}$ symmetry. In the vicinity of AFM instability near half-filling the superconducting temperature T_c reaches values of the order $0.02t \simeq 60$ K. Quasiparticle and spin fluctuation spectra in the normal and superconducting states, calculated also on the real frequency axis by Dahm and Tewordt [37], reveal strong dependence of the spectra on temperature and a strong feedback effect for the effective interactions arising from the spin and charge susceptibilities as the superconducting gap opens. These direct numerical solutions of the strong coupling Eliashberg equations for the Hubbard model in the weak correlation limit unambiguously confirm a possibility of the *d*-wave pairing mediated by the spin fluctuations. However, superconductivity exists only in a narrow range of U, very close to the AFM instability in this model.

In a more rigorous treatment, a self-consistent account of all three types of instability driven by spin or charge density waves or transition into a superconducting state is required. As was shown in a number of investigations within the renormalization group technique, in the two-dimensional generalized $t-t'$ Hubbard model (3), allowing for the next-nearest-neighbor hopping t', several instabilities compete close to half-filling at the Van Hove singularity as was first pointed out by Dzyaloshinskii [41]. An evolution from an AFM instability due to nesting effects at small $t'/t < 0$ over a *d*-wave superconducting pairing at moderate $t'/t \sim -0.3$ to a ferromagnetic ordering at large values of $|t'/t|$ was observed in a one loop approximation in the weak correlation limit $U \sim 3t$ [42]. A phase diagram as a function of the Coulomb interaction U/t and doping was investigated in the original parquet approximation in [43]. The renormalization group technique was also applied to study Fermi surface instability and breakdown of the Landau—Fermi liquid in the two-dimensional $t-t'$ Hubbard model close to half-filling (see, e.g., [44] and the references therein). However, these results obtained in the weak correlation limit $U \sim W/2$ do not lead to a description of the strong-coupling phases revealing only a complicated competition between different types of instability.

Thus, in the framework of the Landau—Fermi liquid model (in the weak correlation limit) the electronic interaction mediated by AFM spin fluctuations can lead to a superconducting pairing. The magnetic pairing mechanism is most effectively manifested itself in the *d*-channel where the local Coulomb repulsion is suppressed. In spite of the pair-breaking effects due to spin scattering which considerably decreases T_c strong enhancement of the spin susceptibility near the AFM instability results in the *d*-wave pairing. An exceptionally strong suppression of T_c in all cuprates by nonmagnetic Zn impurities which are also detrimental to the local magnetic order and in this way suppress the effective spin-fluctuation pairing, provides a «smoking gun» for the magnetic mechanism [17].

1.2.2. Strong correlation limit

Finite cluster calculations. To deal with the strong correlation limit for the Hubbard model and the t–J model a number of numerical methods for finite clusters has been developed (for a review see [12,45–47]). These studies have revealed strong AFM correlations and tendency to the formation of the $d_{x^2-y^2}$ pairing correlations. However, the finite cluster calculations due to known limitations can give only restricted information and usually show contradictory results. For instance, by applying the constrained-path Monte Carlo method [48] to the two-dimensional Hubbard model $d_{x^2-y^2}$ pairing correlations were detected for small size lattices and a weak interaction while with increasing of the lattice sizes or the interaction, they vanished. Close results were also obtained for the t–J model [49]. In later studies pronounced $d_{x^2-y^2}$ pairing correlations were found for the t–J model [50], while for the original Hubbard model no long-range pairing correlation were observed [51]. It seems that for the t–J model the *d*-wave pairing correlations are much easy to detect since they already emerge in the mean-field approximation (MFA) while in the Hubbard model in MFA one gets a very complicated anomalous pairing function (see Sec. 2.2). So to prove the superconducting pairing in the strong correlation limit, an analytical treatment is highly demanded.

Slave-boson representation. To take into account the kinematic interaction caused by the projected character of the electron operators in the t–J model (4), different types of slave-boson (-fermion) technique were proposed (see, e.g., [52–58] and references therein). In the simplest version of the slave-boson theory the projected electron operators $\tilde{a}_{i\sigma}^+$ in (4) are replaced by a product of fermion (spinon) $f_{i\sigma}^+$ and boson (holon) b_i operators: $\tilde{a}_{i\sigma}^+ = f_{i\sigma}^+ b_i$. However, to reduce the enlarged Hilbert space of the spinon-holon particles to the physical one of the projected electron operators one has to introduce a local constraint

$$q_i = b_i^+ b_i + \sum_\sigma f_{i\sigma}^+ f_{i\sigma} = 1. \quad (7)$$

In MFA the local constraint are substituted by a global one, $q = \langle q_i \rangle = 1$ that reduces the problem to free spinons and bosons in the mean-field. The decoupling of spin and charge degrees of freedom in the slave-boson theory results also in quite a different description of the superconducting phase transition by two order parameters, a bose-condensate expectation value $\langle b_i \rangle$, and a spinon pairing function, $\langle f_{i\sigma}^+ f_{j,-\sigma}^+ \rangle$, instead of one order parameter for the original model, $\langle \tilde{a}_{i\sigma}^+ \tilde{a}_{j,-\sigma}^+ \rangle$.

The enlargement of the Hilbert space in the slave-boson (-fermion) representation results in controversial representations for basic physical parameters. For instance, let us consider the slave-fermion hard-core (CP^1) boson representation proposed in [54]. To decouple the charge and spin degrees of freedom for physical electrons in the theory [54] the projected electron operators are represented as a product of a spinless fermion h_i^+ for the charge degree of freedom (holon) and a hard-core boson $b_{i\sigma}$ for the spin degree of freedom (spinon): $\tilde{a}_{i\sigma}^+ = h_i b_{i\sigma}^+$, $\tilde{a}_{i\sigma} = h_i^+ b_{i\sigma}$. This representation has some advantage over other axillary field representations since the constraint of no double occupancy can be fulfilled without introducing the Lagrange multiplier. The hard-core bosons $b_{i\sigma}^+$ are anticommute on the same lattice site prohibiting double occupancy:

$$\sum_\sigma \tilde{a}_{i\sigma}^+ \tilde{a}_{i\sigma} = h_i h_i^+ \sum_\sigma b_{i\sigma}^+ b_{i\sigma} = 1 - h_i^+ h_i \le 1, \quad (8)$$

since $\sum_\sigma b_{i\sigma}^+ b_{i\sigma} = 1$. However, the spin-charge separation imposed by this representation results in extra degrees of freedom: a spin $1/2$ is assigned to any lattice site including an empty site, while for the projected electron operators we have only 3 states: an empty state and a filled state with spin $\pm 1/2$. To cure this defect one should introduce a projection operator to exclude the unphysical states [54]. Otherwise the commutation relations for the original projected electron operators and their representation give different results. The double counting of empty sites results also in controversial equations for an average number of electrons which is valid only with an accuracy of $\pm\delta$ and for a violation of the sum rule for the single-electron Green function (for details see [55]).

To treat the constraint in a systematic way a large-N expansion was proposed [56,57] with $N/2$ being a number of states (orbitals) at a lattice cite. In that approach the local constraint (7) are relaxed to a much weaker one, $q_i = b_i^+ b_i + \sum_\sigma f_{i\sigma}^+ f_{i\sigma} = N/2$. By using the $1/N$ expansion, the d-wave superconducting instability induced by the superexchange interaction was detected in the generalized t–J model close to half filling [58]. The $1/N$ expansion was also used within the Baym – Kadanoff variation technique for the Green functions in terms of the Hubbard operators in [59,60] to study superconducting pairing in the t–J model. It was observed that in the lowest order of $1/N$ there is a strong compensation of different contributions to the pairing interaction and for infinite U ($J = 0$) the superconducting T_c is extremely small [59]. For a finite exchange interaction J the d-wave superconducting instability mediated by the exchange and spin- and charge-fluctuations was obtained below $T_c \simeq 0.01t$ [60]. It was also proved that the results in the Hubbard operator technique differs from that one in the slave-boson representation even in the same order of $1/N$ expansion due to different Hilbert spaces used in two cases. In the limit of large N the kinematic interaction, as in the slave-boson method, is suppressed. This results, in particular, in suppression of the spin-fluctuation contribution which is of the order $1/N$ in comparison with the charge-fluctuation one. Therefore, this approach, being rigorous in the limit $N \to \infty$, is difficult to extrapolate to real spin systems with $N = 2$ where the spin-fluctuation pairing contribution plays the major role.

Spin-polaron model. Important analytical results for the t–J model were obtained in the limit of small concentrations of holes when one can consider the motion of holes on the AFM background within the spin-polaron model [61,62]. A number of studies of this model (see [63–67] and references therein) predicts that a doped hole dressed by strong AFM spin fluctuations can propagate coherently as a QP, spin-polaron, on one of the two AFM sublattices (with spin up and down) in a narrow band of the order J even for a finite hole doping [65,66]. It was natural to suggest that the same spin fluctuations could mediate a superconducting pairing of the spin polarons.

This problem was treated in the framework of the weak coupling BCS formalism. Simple phenomenological models of QP with numerically evaluated spectrum and effective pairing interaction in the atomic limit [68] or mediated by AFM magnon exchange [69] were studied. By applying the rigid band approximation high superconducting transition temperature was obtained for the d-wave pairing. However, since the pairing spin-fluctuation energy J is of the same order as the QP band width the weak coupling BCS equation is inadequate to treat the problem. Also the rigid band approximation for QP fails to describe a strong doping dependence of the QP spectrum [65,66].

A self-consistent numerical treatment of the strong coupling equations for the Green functions and the self-energy for spin-polarons in the t–J model was given in [70]. It was observed a strong renormalization of the QP hole spectrum due to spin-fluctuations and d-wave singlet pairing of two holes on different AFM sublattices with maximum $T_c \simeq 0.01t$ at optimal concentration of doped holes $\delta \simeq 0.2$. In [71] the authors have to introduce an additional electron-phonon coupling to obtain superconducting instability. However, a two-sublattice representation used in the spin-polaron model can be rigorously proved only for a small doping within the long-range AFM state.

Variational approach. To overcome the complicated commutation relations for the original projected electron operators, a variational approach was proposed for the t–J model [72] within the resonance valence bond ground state (see [73] and the references therein). The basic idea in this variational theory was to approximate the original model (4) by a renormalized Hamiltonian for the conventional electron Fermi operators but with the renormalized hopping parameter $\tilde{t} = g_t t$ and the superexchange AFM interaction $\tilde{J} = g_J J$. By using the Gutzwiller variational wave function these variational parameters were estimated in [72] as follow: $g_t = 2\delta/(1+\delta)$, $g_J = 4/(1+\delta)^2$. However, this approach in the limit of low hole concentration $\delta \to 0$, gives the four times larger exchange interaction, $\tilde{J} \simeq 4J$ for the spin-1/2 Heisenberg model which casts doubts on the validity of this simple approximation. A more accurate numerical calculations for the variational wave function in the form of the Gutzwiller projected BCS wave function was performed in [74]. The authors performed extensive numerical studies of superconducting properties of cuprates which appeared in quantitative agreement with experimental data. A certain deficiency of the method, as of any variational approach, is an introduction of a particular variational wave function which may be far away from the real ground state of the complicated system under consideration.

Diagram technique. A rigorous method to treat the unconventional commutation relations for the projected electron operators in the t–J model (4) is based on the Hubbard operator technique [75] since in this representation the local constraint (7) are rigorously implemented by the Hubbard operator algebra. A superconducting pairing due to the kinematic interaction in the Hubbard model in the limit of strong electron correlations ($U \to \infty$) was first obtained by Zaitsev and Ivanov [76] who studied the two-particle vertex equation by applying a diagram technique for Hubbard operators. However, they studied only the lowest order diagrams which are equivalent to MFA for a superconducting order parameter and obtained only the **k**-independent s-wave pairing.

Systematic investigation of the t–J model within the diagram technique was performed by Izymov et al. [77]. In the framework of this approach spin fluctuations and superconducting pairing in the t–J model in the limit of small J were studied in [78,79]. The first order diagrams for the self-energy reproduced the results of MFA obtained by the projection technique for the thermodynamic Green function in [80]. In calculations of the second order diagrams only the exchange interaction J was taken into account while the corresponding contributions due to the kinematic interaction of the order t^2 was disregarded which is in fact gives a large contribution to the spin-fluctuation pairing [81]. As a result, estimations in the weak coupling limit for the Eliashberg equation for a three-dimensional model near AFM instability resulted in quite a low superconducting T_c.

Equation of motion method for the Green functions. The equation of motion method for the thermodynamic Green functions [82] appears to be much more simple than the diagram technique. To overcome the problem of uncontrollable decoupling procedure in the method, one should use the Mori-type projection technique which has proved to be quite accurate for systems with strong correlations. For instance, as has been demonstrated in [83], this approach accurately reproduces the results of the diagram technique for the spin-1/2 Heisenberg model within the second order of the exchange interaction for the self-energy.

At first superconducting pairing was considered for the Hubbard model in [84,85] by applying a decoupling procedure within the equation of motion method for the Green functions. The s-wave pairing due to the kinematic interaction proposed in [76] was obtained in MFA-type approximation. However, as was shown later [80], the s-wave pairing in the limit of strong correlations violates an exact requirement of no single-site pairs and should be disregarded. The BCS-type theory for the t–J model was developed in [80] within the projection technique for the Green functions in terms of the Hubbard operators. It was proved in MFA that the d-wave superconducting pairing mediated by the exchange interaction J is stable and has high $T_c \simeq 0.1t$ for $J \simeq 0.4t$. Later on, T_c dependence on the in-plane lattice constant (or pressure) and the oxygen isotope shift were studied [86]. The theory of electron spectra and superconducting pairing beyond MFA was formulated for the t–J model in [81] by self-consistent solution of the Dyson equation within the noncrossing approximation for

the matrix self-energy (see Sec. 3). Our results for the effective p–d Hubbard model [87–89] and studies of superconducting pairing in the original Hubbard model (3) by several authors [90–92] by the equation of motion method are considered in the next Section.

2. Superconducting pairing in the p–d Hubbard model

As we discussed above, studies of the reduced one-band t–J model have demonstrated that the AFM exchange interaction already in the MFA mediates the d-wave pairing with a high T_c. To go beyond the MFA, one has to consider the original two-band p–d model for CuO_2 layer without reduction the interband hopping to an effective instantaneous exchange interaction in the t–J model. The same problem emerges when instead of an instantaneous pairing interaction in the BCS model one studies an original electron-phonon interaction in the Eliashberg equation. In this case retardation effects in the electron-phonon interaction result in restriction of the pairing attraction within a narrow energy shell of the order of phonon frequency close to the Fermi surface. In this section we describe a microscopic theory of superconductivity within the effective p–d Hubbard model and demonstrate that the retardation effects in the exchange interaction are negligible, while in the spin-fluctuation pairing they are important and cut off the attraction by the characteristic spin-fluctuation energy $\omega_s \sim J$.

The superconducting properties of metals are principally defined by their electronic structure in the normal state. Therefore it is essential to determine the latter before studying a mechanism of superconductivity. Electronic spectrum and nature of charge carriers in the cuprate superconductors have been extensively discussed but it is still a controversial problem. First of all, a lot of numerical calculations within the LDA method should be mentioned (see, e.g., [93,94] and the references therein) which, however, failed to reproduce a charge-transfer insulating phase of undoped cuprate compounds. Therefore, a more sophisticated methods were developed as LDA + U method (for a review see [95]). Based on these investigations, a simplified model for analytical analysis of the low-energy part of electronic spectrum can be constructed [94]. To take into account the most important oxygen p_x, p_y and copper $3d_{x^2-y^2}$ orbitals in CuO_2 layers and strong Coulomb correlations in the unit cell, a p–d model was proposed originally by Emery [96] and Varma et al. [97]. A more general many-band model was considered by Gaididei and Loktev [98]. However, to be able to treat many-band models analytically, one has to simplify them further to keep only the lowest electron excitations close to the Fermi surface.

There are generally two different types of approach to the problem. In the first one, the Bloch representation for the oxygen and copper hole wave functions are used that results in appearance of two bands of oxygen and copper states (see, e.g., [99] and the references therein). In this case no singlet-triplet splitting occurs since the $pd\sigma$ hybridization vanishes in the Bloch representation at the center of the Brillouin zone, at $\mathbf{k} = 0$. Therefore a spin direction of an oxygen hole will be frustrated and, as was shown within a two-level spin model for an oxygen hole between two copper sites by Maleev [100], a strong spin scattering of oxygen holes on copper spins *in a single unit cell* will prevent formation of oxygen coherent quasiparticles. This scattering is usually neglected in construction of oxygen hole QPs in ionic models within the Bloch wave-function representation.

In another approach local basis set of the oxygen and copper wave functions is used since the $pd\sigma$ hybridization t_{pd} is so strong that instead of free doped oxygen holes the $pd\sigma$ Zhang–Rice singlet (ZRS) states appear [101]. To derive ZRS state one should start from the local representation for the oxygen Wannier states around the Cu-site to take into account strong exchange interaction of the order of 1 eV between the copper and oxygen holes *in a single unit cell*. A perturbation theory over t_{pd} / Δ_{pd} in this case (used originally in [101]) is not justified (the charge transfer gap $\epsilon_p - \epsilon_d = \Delta_{pd} \sim 2t_{pd}$) and a direct diagonalization of these local states should be performed. In exact diagonalization for electronic states for a single site Hamiltonian, all the Coulomb interactions in a single unit cell, not only U_{dd}, but also U_{pp}, V_{pd} along with the oxygen hole hopping matrix element t_{pp} can be taken into account rigorously (see, e.g., [87,102] and the references therein). This *cell cluster perturbation theory* was also extensively studied by applying exact numerical diagonalization by Feiner et al. [103] who have shown an efficiency of this method. It provides a proper perturbation theory over a small intercell hopping, $t_{i \neq j} \sim 0.1 t_{pd}$, which results from a small overlapping of the local oxygen Wannier states in the neighboring unit cells. Therefore, to take into account strong spin correlations between oxygen and copper holes and to derive a *coherent* spectrum of QPs in the CuO_2 plane it is very important to start from a proper basis for the wave functions: not extended Bloch waves but localized states in a single unit cell.

2.1. Dyson equation

By applying the sell-cluster perturbation theory cited above we can reduce the original two-band p–d model for CuO_2 layer to an effective two-band Hubbard model with the lower Hubbard subband (LHB) occupied by one-hole Cu d-like states and the upper Hubbard subband (UHB) occupied by the two-hole ZRS states. In terms of the Hubbard operators the model reads:

$$H = \varepsilon_1 \sum_{i,\sigma} X_i^{\sigma\sigma} + \varepsilon_2 \sum_i X_i^{22} + \sum_{i \neq j,\sigma} \Big\{ t_{ij}^{11} X_i^{\sigma 0} X_j^{0\sigma} + t_{ij}^{22} X_i^{2\sigma} X_j^{\sigma 2} + 2\sigma t_{ij}^{12} (X_i^{2\overline{\sigma}} X_j^{0\sigma} + \text{h.c.}) \Big\}, \quad (9)$$

where $X_i^{nm} = |in\rangle\langle im|$ are the Hubbard operators for the four states $n,m = |0\rangle, |\sigma\rangle, |2\rangle = |\uparrow\downarrow\rangle$, $\sigma = \pm 1/2 = (\uparrow, \downarrow)$, $\overline{\sigma} = -\sigma$. Here $\varepsilon_1 = \varepsilon_d - \mu$ and $\varepsilon_2 = 2\varepsilon_1 + \Delta$ are the single-site energy where μ is the chemical potential and $\Delta = \epsilon_p - \epsilon_d$ is the charge transfer gap which plays the role of U in the conventional Hubbard model (3). The superscript 2 and 1 refers to the singlet UHB and the one-hole LHB, respectively. The hopping integrals are given by $t_{ij}^{\alpha\beta} = K_{\alpha\beta} \cdot 2t\nu_{ij}$, where t is the p–d hybridization parameter and ν_{ij} are estimated as: $\nu_1 = \nu_{j\, j \pm a_{x/y}} \simeq -0.14$, $\nu_2 = \nu_{j\, j \pm a_x \pm a_y} \simeq -0.02$ (see [87]). The coefficients $K_{\alpha\beta} \sim 0.5$ take into account the p–d hybridization in a single unit cell. Therefore, the effective hopping parameter $t_{\text{eff}} \sim K_{22} \cdot 2t\nu_1 \sim 0.14t$ are small and for the bandwidth $W = 8t_{\text{eff}} \sim 1.12t$ we get the ratio $W/\Delta \sim 1/2$ for the standard parameters $\Delta \sim 2t \simeq 3$ eV. This shows that the Hubbard model (9) corresponds to the strong correlation limit. The chemical potential μ depends on the average electron occupation number

$$n = \langle N_i \rangle = \sum_\sigma \langle X_i^{\sigma\sigma} \rangle + 2\langle X_i^{22} \rangle, \quad (10)$$

where N_i is the number operator. The Hubbard operators entering (9) obey the completeness relation

$$X_i^{00} + X_i^{\uparrow\uparrow} + X_i^{\downarrow\downarrow} + X_i^{22} = 1, \quad (11)$$

which rigorously preserves the constraint of no double occupancy of any quantum state $|in\rangle$ at each lattice site i.

It is important to point out that interaction of charge carriers with spin or charge fluctuations comes from the nonfermionic commutation relations of the Hubbard operators (kinematic interaction). This can be seen explicitly, for example, from the commutation relations for the hopping term

$$[X_i^{0\sigma}, \sum_{l \neq m,\sigma'} t_{lm} X_l^{\sigma' 0} X_m^{0\sigma'}] = \sum_{l,\sigma'} t_{il} B_{i\sigma\sigma'} X_l^{0\sigma'}. \quad (12)$$

Here the Bose-like operator is introduced

$$B_{i\sigma\sigma'} = (X_i^{00} + X_i^{\sigma\sigma})\delta_{\sigma'\sigma} + X_i^{\overline{\sigma}\sigma}\delta_{\sigma'\overline{\sigma}} = (1 - \frac{1}{2}N_i + 2\sigma S_i^z)\delta_{\sigma'\sigma} + S_i^{\overline{\sigma}}\delta_{\sigma'\overline{\sigma}}, \quad (13)$$

which is defined by the number and spin operators as follows from (11). Therefore, the hopping probability of an electron in the Hubbard model depends on the spin and charge states of the lattice site which results in a renormalization of the electronic spectrum due to this kinematic interaction.

To discuss the superconducting pairing within the model Hamiltonian (9), we introduce the four-component Nambu operators $\hat{X}_{i\sigma}$ and $\hat{X}_{i\sigma}^\dagger$ and define the thermodynamic 4×4 matrix Green function (GF) [82]

$$\tilde{G}_{ij\sigma}(t - t') = \langle\langle \hat{X}_{i\sigma}(t) | \hat{X}_{j\sigma}^\dagger(t') \rangle\rangle,$$
$$\tilde{G}_{ij\sigma}(\omega) = \begin{pmatrix} \hat{G}_{ij\sigma}(\omega) & \hat{F}_{ij\sigma}(\omega) \\ \hat{F}_{ij\sigma}^\dagger(\omega) & -\hat{G}_{ji\overline{\sigma}}(-\omega) \end{pmatrix}, \quad (14)$$

where $\hat{X}_{i\sigma}^\dagger = (X_i^{2\sigma} \;\; X_i^{\overline{\sigma}0} \;\; X_i^{\overline{\sigma}2} \;\; X_i^{0\sigma})$ and $\hat{G}_{ij\sigma}$ and $\hat{F}_{ij\sigma}$ are normal and anomalous 2×2 matrix components, respectively. By applying the projection technique for equation of motion method for GF (14), we derive the Dyson equation in $(\mathbf{q},\omega)$-representation [88]:

$$(\tilde{G}_\sigma(\mathbf{q},\omega))^{-1} = (\tilde{G}_\sigma^0(\mathbf{q},\omega))^{-1} - \tilde{\Sigma}_\sigma(\mathbf{q},\omega),$$
$$\tilde{G}_\sigma^0(\mathbf{q},\omega) = (\omega\tilde{\tau}_0 - \tilde{E}_\sigma(\mathbf{q}))^{-1}\tilde{\chi}, \quad (15)$$

where $\tilde{\tau}_0$ is the 4×4 unity matrix and $\tilde{\chi} = \langle\{\hat{X}_{i\sigma}, \hat{X}_{i\sigma}^\dagger\}\rangle$. The zero-order GF $\tilde{G}_\sigma^0(\mathbf{q},\omega)$ within the generalized MFA is defined by the frequency matrix which in the site representation reads

$$\tilde{E}_{ij\sigma} \cong \tilde{\mathcal{A}}_{ij\sigma}\tilde{\chi}^{-1}, \;\; \tilde{\mathcal{A}}_{ij\sigma} = \langle\{[\hat{X}_{i\sigma}, H], \hat{X}_{j\sigma}^\dagger\}\rangle, \quad (16)$$

where $\{A,B\} = AB + BA$, $[A,B] = AB - BA$. The self-energy operator in the Dyson equation (15) in the projection technique method is defined by a *proper* part (having no single zero-order GF) of the many-particle GF in the form

$$\tilde{\Sigma}_\sigma(\mathbf{q},\omega) = \tilde{\chi}^{-1}\langle\langle \hat{Z}_\sigma^{(\text{ir})} | \hat{Z}_\sigma^{(\text{ir})\dagger} \rangle\rangle_{\mathbf{q},\omega}^{(\text{prop})}\tilde{\chi}^{-1}. \quad (17)$$

Here the *irreducible* $\hat{Z}$-operator is given by the equation: $\hat{Z}_\sigma^{(\text{ir})} = [\hat{X}_{i\sigma}, H] - \sum_l \tilde{E}_{il\sigma} X_{l\sigma}$ which follows from the orthogonality condition: $\langle\{\hat{Z}_\sigma^{(\text{ir})}, \hat{X}_{j\sigma}^\dagger\}\rangle = 0$. The Eqs. (15)–(17) provide an *exact representation* for the GF (14). However, to calculate it one has to

use approximations for the self-energy matrix (17) which describes the finite lifetime effects.

2.2. Mean-field approximation

In the MFA the electronic spectrum and superconducting pairing are described by the zero-order GF in (15). By applying the commutation relations for the Hubbard operators we get for the frequency matrix (16):

$$\tilde{\mathcal{A}}_{ij\sigma} = \begin{pmatrix} \hat{\omega}_{ij\sigma} & \hat{\Delta}_{ij\sigma} \\ \hat{\Delta}^{*}_{ji\sigma} & -\hat{\omega}_{ji\bar{\sigma}} \end{pmatrix}. \qquad (18)$$

The normal component $\hat{\omega}_{ij\sigma}$ defines quasiparticle spectra $\Omega_{1,2}(\mathbf{q})$ for the two Hubbard subbands of the model in the normal state which have been studied in detail in [87]. As an example, Fig. 1 shows the dispersion $\Omega_{1,2}(\mathbf{q})$ calculated in the paramagnetic state for the parameters $\Delta = 2t = 3$ eV in the model (9). For $n = 1$ an insulating state is observed with the Fermi level (dotted line) being between the subbands. The singlet band dispersion $\Omega_2(\mathbf{q})$ is defined by the next nearest neighbor (n.n.n.) hopping as in the AFM state due to the renormalization of the hopping parameters by the short-range spin correlation functions for the n.n. $\langle \mathbf{S}_i \mathbf{S}_{i \pm a_x / a_y} \rangle$ and the n.n.n. $\langle \mathbf{S}_i \mathbf{S}_{i \pm a_x \pm a_y} \rangle$ sites. With doping, the Fermi level shifts to the singlet subband and for the overdoped case $n = 1.4$ the dispersions are defined by the nearest neighbor (n.n.) hopping since the short-range spin correlation functions are suppressed. This type behavior of dispersions qualitatively agrees with the ARPES experiments.

The anomalous component $\hat{\Delta}_{ij\sigma}$ defines the gap functions for the singlet and one-hole subbands, respectively, $(i \neq j)$:

$$\Delta^{22}_{ij\sigma} = -2\sigma t^{12}_{ij} \langle X^{02}_i N_j \rangle, \; \Delta^{11}_{ij\sigma} = -2\sigma t^{12}_{ij} \langle (2 - N_j) X^{02}_i \rangle . \qquad (19)$$

Using the definitions of the Fermi annihilation operators: $c_{i\sigma} = X^{0\sigma}_i + 2\sigma X^{\bar{\sigma}2}_i$, we can write the anomalous average in (19) as $\langle c_{i\downarrow} c_{i\uparrow} N_j \rangle = \langle X^{0\downarrow}_i X^{\downarrow 2}_i N_j \rangle = \langle X^{02}_i N_j \rangle$ since other products of the Hubbard operators vanish according to the multiplication rule for the Hubbard operators: $X^{\alpha\gamma}_i X^{\lambda\beta}_i = \delta_{\gamma,\lambda} X^{\alpha\beta}_i$. Therefore the anomalous correlation functions in MFA describe the *pairing at one lattice site but in different Hubbard subbands*.

The same anomalous correlation functions were obtained in MFA for the original Hubbard model in Refs. 90–92. To calculate the anomalous correlation function $\langle c_{i\downarrow} c_{i\uparrow} N_j \rangle$ in [90,92] the Roth procedure was applied based on a decoupling of the operators on the same lattice site in the time-dependent correlation function: $\langle c_{i\downarrow}(t) | c_{i\uparrow}(t') N_j(t') \rangle$. However, the decoupling of the Hubbard operators on the same lattice site is not unique (as has been really observed in Refs. 90, 92) and unreliable. To escape uncontrollable decoupling, in Ref. 91 kinematical restrictions imposed on the correlation functions for the Hubbard operators were used which, however, also have not produced a unique solution for superconducting equations.

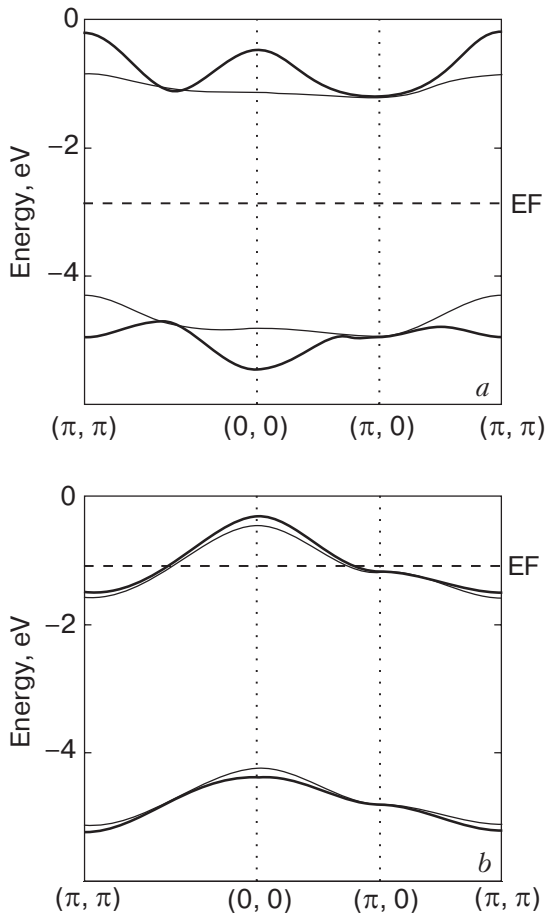

Fig. 1. Hole dispersion curves (solid lines) along the symmetry directions for the half-filled case, $n = 1$ (*a*) and for the overdoped case, $n = 1.4$ (*b*). Thin lines show the dispersions without hybridization ($t^{12}_{ij} = 0$) [87].

In our approach we perform a direct calculation of the correlation function $\langle X^{02}_i N_j \rangle$ without *any decoupling* by writing equation of motion for the corresponding commutator GF $L_{ij}(t - t') = \langle\langle X^{02}_i(t) | N_j(t') \rangle\rangle$ as follows:

$$(\omega - \varepsilon_2) L_{ij}(\omega) \simeq 2\delta_{ij} \langle X^{02}_i \rangle + \sum_{m \neq i, \sigma} 2\sigma \, t^{12}_{im} \left\{ \langle\langle X^{0\bar{\sigma}}_i X^{0\sigma}_m | N_j \rangle\rangle_\omega - \langle\langle X^{\sigma 2}_i X^{\bar{\sigma}2}_m | N_j \rangle\rangle_\omega \right\}, \qquad (20)$$

where we neglected intraband hopping $|t^{\alpha\alpha}_{im}| << \varepsilon_2 \simeq \Delta$. After applying the spectral theorem and ne-

glecting exponentially small terms of the order of $\exp(-\Delta/T) << 1$, we obtain the following representation for the correlation function at sites $i \neq j$ for the singlet subband in the case of hole doping [89]:

$$\langle X_i^{02} N_j \rangle = -\frac{1}{\Delta} \sum_{m \neq i,\sigma} 2\sigma t_{im}^{12} \langle X_i^{\sigma 2} X_m^{\bar{\sigma} 2} N_j \rangle \simeq$$

$$\simeq -\frac{4t_{ij}^{12}}{\Delta} 2\sigma \langle X_i^{\sigma 2} X_j^{\bar{\sigma} 2} \rangle . \qquad (21)$$

The last equation is obtained in the two-site approximation, $m = j$, usually applied for the t–J model. This finally allows us to write the gap function in (19) in the case of hole doping as follows

$$\Delta_{ij\sigma}^{22} = -2\sigma\, t_{ij}^{12} \langle X_i^{02} N_j \rangle = J_{ij} \langle X_i^{\sigma 2} X_j^{\bar{\sigma} 2} \rangle . \quad (22)$$

This result is similar to the exchange interaction contribution to the pairing in the t–J model with the exchange energy $J_{ij} = 4\,(t_{ij}^{12})^2 / \Delta$. In the case of electron doping, an analogous calculation for the anomalous correlation function of the one-hole subband $\langle (2 - N_j) X_i^{02} \rangle$ gives for the gap function $\Delta_{ij\sigma}^{11} = J_{ij} \langle X_i^{0\bar{\sigma}} X_j^{0\sigma} \rangle$. We may therefore conclude that the anomalous contributions to the zero-order GF (15) is just the conventional anomalous pairs of QPs in one subband. Their pairing in MFA is mediated by the exchange interaction which has been studied in the t–J model (see, e.g., [80,81]) and there are no new «composite operator excitations» («cexons») proposed in [92].

2.3. Self-energy and the gap equation

The self-energy matrix (17) can be written in the same form as GF (14):

$$\tilde{\Sigma}_{ij\sigma}(\omega) = \tilde{\chi}^{-1} \begin{pmatrix} \hat{M}_{ij\sigma}(\omega) & \hat{\Phi}_{ij\sigma}(\omega) \\ \hat{\Phi}^{\dagger}_{ij\sigma}(\omega) & -\hat{M}_{ij\bar{\sigma}}(-\omega) \end{pmatrix} \tilde{\chi}^{-1}, \quad (23)$$

where the 2×2 matrices $\hat{M}$ and $\hat{\Phi}$ denote the normal and anomalous contributions to the self-energy, respectively. The self-energy (23) is calculated below in the non-crossing or the self-consistent Born approximation (SCBA). In the SCBA, the propagation of the Fermi-like $X_j = X_j^{0\sigma}$ $(X_j^{\bar{\sigma} 2})$ and the Bose-like B_i (13) excitations in the many-particle GF in (23) are assumed to be independent of each other. This approximation is given by the decoupling of the corresponding operators in the time-dependent correlation functions for different lattice sites $(i \neq j,\ l \neq m)$ as follows

$$\langle B_i(t) X_j(t) B_l(t') X_m(t') \rangle \simeq$$
$$\simeq \langle X_j(t) X_m(t') \rangle \langle B_i(t) B_l(t') \rangle . \qquad (24)$$

Using the spectral representation for these correlation functions we get a closed system of equations for the GF (14) and the self-energy components (23) [89]. Below we write down explicitly only the anomalous part of the self-energy for the singlet band which is relevant for further discussion:

$$\Phi_{\sigma}^{22}(\mathbf{q},\omega) = \frac{1}{N} \sum_{\mathbf{k}} |t(\mathbf{k})|^2 \int_{-\infty-\infty}^{+\infty+\infty} \frac{d\omega_1 d\omega_2}{\omega - \omega_1 - \omega_2} \times$$

$$\times \frac{1}{2} \left(\tanh \frac{\omega_1}{2T} + \coth \frac{\omega_2}{2T} \right) \chi_s''(\mathbf{q} - \mathbf{k}, \omega_2) \times$$

$$\times \left\{ -\frac{1}{\pi} \operatorname{Im} \left[K_{22}^2 F_{\sigma}^{22}(\mathbf{k},\omega_1) - K_{21}^2 F_{\sigma}^{11}(\mathbf{k},\omega_1) \right] \right\} . \quad (25)$$

The kinematic interaction for the nearest and the second neighbors is given by $t(\mathbf{k}) = t_1(\mathbf{k}) + t_2(\mathbf{k}) = 8t[\nu_1 \gamma(\mathbf{k}) + \nu_2 \gamma'(\mathbf{k})]$, where $\gamma(\mathbf{k}) = (1/2)(\cos k_x + \cos k_y)$ and $\gamma'(\mathbf{k}) = \cos k_x \cos k_y$. The pairing interaction is mediated by spin-fluctuations defined by the susceptibility $\chi_s''(\mathbf{q},\omega) = -(1/\pi) \operatorname{Im} \langle\langle \mathbf{S}_q | \mathbf{S}_{-q} \rangle\rangle_{\omega + i\delta}$ which comes from the correlation functions $\langle B_i(t) B_l(t') \rangle$ in (24) in terms of the Bose-like operators (13).

For the hole doped case, at frequencies $|\omega, \omega_1| << \omega_s << W$ close to the Fermi surface (FS) ($\omega_s \leq J$ is a characteristic spin-fluctuation energy) we can use the weak coupling approximation (WCA) for calculation of the first term in the self-energy (25). The contribution from the second term $F_{\sigma}^{11}(\mathbf{k},\omega_1)$ is rather small since the one-hole band lies below the FS at the energy of the order $\Delta >> W$. Neglecting it and taking into account the contribution from the exchange interaction in MFA (22), we arrive at the following equation for the superconducting gap at the FS in the singlet subband:

$$\Phi^{22}(\mathbf{q}) = \frac{1}{N} \sum_{\mathbf{k}} [J(\mathbf{k} - \mathbf{q}) - K_{22}^2\ \lambda(\mathbf{k}, \mathbf{q} - \mathbf{k})] \times$$

$$\times \frac{\Phi^{22}(\mathbf{k})}{2E_2(\mathbf{k})} \tanh \frac{E_2(\mathbf{k})}{2T} , \qquad (26)$$

where $\lambda(\mathbf{k}, \mathbf{q} - \mathbf{k}) = |t(\mathbf{k})|^2\, \chi_s(\mathbf{q} - \mathbf{k}, \omega = 0) > 0$. The quasiparticle energy in the singlet band is given by $E_2(\mathbf{k}) = \{[\Omega_2(\mathbf{k})]^2 + [\Phi^{22}(\mathbf{k})]^2\}^{1/2}$ where $\Omega_2(\mathbf{k})$ is the quasiparticle energy in the normal state (see Fig. 1). Similar considerations hold true for an electron doped system, $n \leq 1$ when the chemical potential lies in the one-hole band, $\mu \simeq 0$. In that case, the WCA equation for the gap $\Phi^{11}(\mathbf{q})$ is quite similar to (26).

To solve the gap equation (26) we used the following model for the static spin-fluctuation susceptibility: $\chi_s(\mathbf{q},0) = \chi_0 / \{1 + \xi^2 [1 + \gamma(\mathbf{q})]\}$ where ξ is

the AFM correlation length and the constant $\chi_0 = 3(1-\delta)/(2\pi\omega_s C_1)$ with $C_1 = (1/N)\sum_{\mathbf{q}}\{1+\xi^2[1+\gamma(\mathbf{q})]\}^{-1}$ is defined from the normalization condition: $(1/N)\sum_i \langle \mathbf{S}_i \mathbf{S}_i \rangle = (3/4)(1-\delta)$. Let us at first estimate the superconducting transition temperature T_c by solving the gap equation (26) for a model d-wave gap function $\Phi^{22}(\mathbf{q}) = \varphi_d(\cos q_x - \cos q_y) \equiv \equiv \varphi_d \eta(\mathbf{q})$ in the standard logarithmic approximation in the limit of weak coupling. Integration over $\mathbf{q}$ both sides of (26) multiplied by $\eta(\mathbf{q})$ results in the following equation for T_c:

$$1 = \frac{1}{N}\sum_{\mathbf{k}} [J\eta^2(\mathbf{k}) + \lambda_s (4\gamma(\mathbf{k}))^2 \eta^2(\mathbf{k})] \times \times \frac{1}{2\Omega_2(\mathbf{k})} \tanh \frac{\Omega_2(\mathbf{k})}{2T_c}, \qquad (27)$$

where $\lambda_s \simeq t_{\text{eff}}^2/\omega_s$. For the first term — the exchange interaction mediated by the interband hopping, the retardation effects are negligible that results in coupling of all electrons in a broad energy shell of the order of the bandwidth W and high T_c [86]:

$$T_c \simeq \sqrt{\mu(W-\mu)} \exp(-1/\lambda_{\text{ex}}), \qquad (28)$$

where $\lambda_{\text{ex}} \simeq JN(\delta)$ is an effective coupling constant for the exchange interaction J and the average density $N(\delta)$ of electronic states for doping δ. For the second term in (26), the spin-fluctuation pairing mediated by the intraband hopping, the interaction is restricted by a narrow energy shell $\pm\omega_s$ at the FS which results in $T_c \propto \omega_s$. By taking into account the both contributions, we can write the following estimation for T_c:

$$T_c \simeq \omega_s \exp\left(-\frac{1}{\tilde{\lambda}_{sf}}\right), \qquad \tilde{\lambda}_{sf} = \lambda_{sf} + \frac{\lambda_{\text{ex}}}{1-\lambda_{\text{ex}} \ln(\mu/\omega_s)}, \qquad (29)$$

where $\lambda_{sf} \simeq \lambda_s N(E_F)$ is the coupling constant for the spin-fluctuation pairing. By taking for estimation $\mu = W/2 \simeq 0.35$ eV, $\omega_s \simeq J \simeq 0.13$ eV and $\lambda_{sf} \simeq \lambda_{\text{ex}} = 0.2$ we get $\tilde{\lambda}_{sf} \simeq 0.2 + 0.25 = 0.45$ and $T_c \simeq 160$ K, while only the spin-fluctuation pairing gives $T_c^0 \simeq \omega_s \exp(-1/\lambda_{sf}) \simeq 10$ K.

Results of a direct numerical solution of the gap equation (26) are shown in Fig. 2 for the superconducting transition temperature $T_c(\delta)$ and the gap $\Phi^{22}(\mathbf{k})$ [89]. The following parameters are used: $\xi = 3$, $J = 0.4t_{\text{eff}}$, $\omega_s = 0.15$ eV and $t_{\text{eff}} = K_{22} 2tv_1 \simeq 0.2$ eV. The maximum $T_c \sim 280$ K (dotted line) is achieved for the chemical potential $\mu = E_F \simeq W/2$ at the optimal doping $\delta_{\text{opt}} \simeq 0.12$. The spin-fluctuation interaction produces lower T_c (solid line) since it is rather weak at the FS close to the AF zone boundary along the lines $|k_x| + |k_y| = \pi$ where the main contribution coming from the n.n. hopping vanishes: $t_1(\mathbf{k}) \propto \gamma(k_x, |k_y| = \pi - |k_x|) = 0$.

We can confirm the AFM pairing mechanism by considering T_c dependence on pressure or lattice constants. While in electron-phonon superconductors T_c decreases under pressure, in cuprates T_c increases with compression of the in-plane lattice constant a. In particular, in mercury superconductors $dT_c/da \simeq -1.35 \cdot 10^3$ K/Å [104] and for Hg-1201 compound

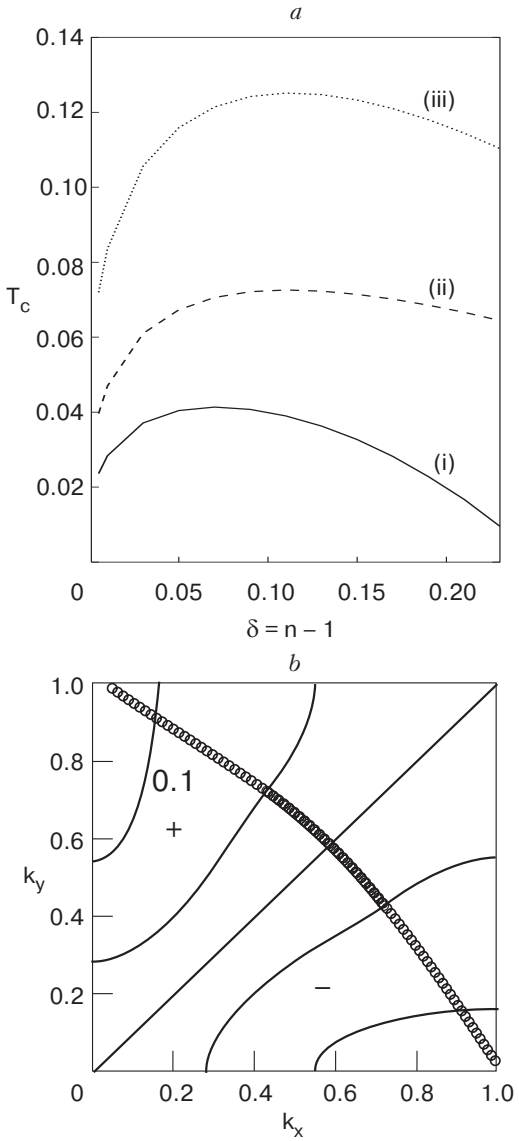

Fig. 2. (*a*) Superconducting $T_c(\delta)$ (in units of $t_{\text{eff}} \simeq 0.2$ eV) for (i) spin-fluctuation interaction (solid line), (ii) exchange interaction (dashed line), (iii) for the both contributions (dotted line). (*b*) Wave-vector dependence of the gap function $\Phi^{22}(\mathbf{k})$ over the first quadrant of the BZ ($\delta = 0.13$). The circles plot the Fermi surface. The (+/–) denote gap signs inside the octants [89].

we get $d\ln T_c / d\ln a \simeq -50$. From (28) we get an estimate:

$$\frac{d\ln T_c}{d\ln a} \simeq \frac{d\ln T_c}{d\ln J}\frac{d\ln J}{d\ln a} \simeq -\frac{14}{\lambda} \simeq -47 \qquad (30)$$

which is quite close to the experimentally observed one. Here we use $\lambda = JN(\delta) \simeq 0.3$ and take into account that for the exchange interaction we can use an estimate $J(a) \propto t_{pd}^4$ where $t_{pd} \propto 1/a^{7/2}$ for the p–d hybridization.

Concerning an oxygen isotope effect in cuprates, on substitution ^{18}O oxygen for ^{16}O, we can estimate it also from (28). By using the experimentally observed isotope shift for the Néel temperature in La_2CuO_4 [105]: $\alpha_N = -(d\ln T_N / d\ln M) \simeq (d\ln J / d\ln M) \simeq$ $\simeq 0.05$ we obtain

$$\alpha_c = -\frac{d\ln T_c}{d\ln M} = -\frac{d\ln T_c}{d\ln J}\frac{d\ln T_N}{d\ln M} \simeq \frac{\alpha_N}{\lambda} \simeq 0.16\ , \qquad (31)$$

for $\lambda \simeq 0.3$ which is close to experiments: $\alpha_c = -d\ln T_c / d\ln M \le 0.1$. As we see, we can explain qualitatively experimental data in superconducting state of cuprates within the proposed theory based on the effective p–d model with only two fitting parameters, Δ and $t = t_{pd}$, used in the calculations of the electron dispersion in the normal state.

3. Superconducting pairing in t–J model

It is interesting to compare the results of the original two-band p–d model for CuO_2 layer (9) with the calculations for the t–J in Ref. 81. In that paper, a full self-consistent numerical solution for the normal and anomalous GF in the Dyson equation was performed in the strong-coupling limit. The QP renormalization and finite life-time effects caused by the self-energy operators which were neglected in the above calculations were fully taken into account.

In the limit of strong correlations the interband hopping in the model (9) can be excluded by perturbation theory which results in the effective t–J model (4) which can written in terms of the Hubbard operator as follow:

$$H_{t-J} = -\sum_{i\ne j,\sigma} t_{ij} X_i^{\sigma 0} X_j^{0\sigma} - \mu \sum_{i\sigma} X_i^{\sigma\sigma} + \\ + \frac{1}{4}\sum_{i\ne j,\sigma} J_{ij}\left(X_i^{\sigma\bar\sigma} X_j^{\bar\sigma\sigma} - X_i^{\sigma\sigma} X_j^{\bar\sigma\bar\sigma}\right), \qquad (32)$$

where only the lower Hubbard subband is considered with the hopping energy t_{ij}. Exclusion of the interband hopping results in the instantaneous exchange interaction $J_{ij} = 4\,(t_{ij}^{12})^2 / \Delta$. The superconducting pairing within the model (32) can be studied by considering the matrix GF for the lower Hubbard subband in terms of the Nambu operators: $\Psi_{i\sigma}$ and $\Psi_{i\sigma}^+ = (X_i^{\sigma 0}; X_i^{0\bar\sigma})$:

$$\hat G_{ij,\sigma}(t-t') = \langle\langle \Psi_{i\sigma}(t) | \Psi_{j\sigma}^+(t')\rangle\rangle, \\ \hat G_{ij\sigma}(\omega) = Q \begin{pmatrix} G_{ij\sigma}^{11}(\omega) & G_{ij\sigma}^{12}(\omega) \\ G_{ij\sigma}^{21}(\omega) & G_{ij\sigma}^{22}(\omega) \end{pmatrix}. \qquad (33)$$

Here we introduced the Hubbard factor $Q = 1 - n/2$ depending on the average number of electrons $n = \sum_\sigma \langle X_i^{\sigma\sigma}\rangle$. By applying the projection technique as described above we get the Dyson equation which can be written in the Eliashberg notation as

$$\hat G_\sigma(\mathbf{k},\omega) = Q\frac{\omega Z_\sigma(\mathbf{k},\omega)\hat\tau_0 + [E_\sigma(\mathbf{k}) + \xi_\sigma(\mathbf{k},\omega) - \tilde\mu]\hat\tau_3 + \Phi_\sigma(\mathbf{k},\omega)\hat\tau_1}{[\omega Z_\sigma(\mathbf{k},\omega)]^2 - [E_\sigma(\mathbf{k}) + \xi_\sigma(\mathbf{k},\omega) - \tilde\mu]^2 - |\Phi_\sigma(\mathbf{k},\omega)|^2}\ , \qquad (34)$$

where $\hat\tau_i$ are the Pauli matrices. The quasiparticle energy $E_\sigma(\mathbf{k})$ in the normal state and the renormalized chemical potential $\tilde\mu = \mu - \delta\mu$ are calculated in MFA as discussed above (for details see [81]). The frequency-dependent functions

$$\omega(1 - Z_\sigma(\mathbf{k},\omega)) = \frac{1}{2}[\Sigma_\sigma^{11}(\mathbf{k},\omega) + \Sigma_\sigma^{22}(\mathbf{k},\omega)],$$

$$\xi_\sigma(\mathbf{k},\omega) = \frac{1}{2}[\Sigma_\sigma^{11}(\mathbf{k},\omega) - \Sigma_\sigma^{22}(\mathbf{k},\omega)]$$

are defined by the normal components of the self-energy $\Sigma_\sigma^{22}(\mathbf{k},\omega) = -\Sigma_{\bar\sigma}^{11}(\mathbf{k},-\omega)$. The gap function is specified by the equation:

$$\Phi_\sigma(\mathbf{k},\omega) = \Delta_\sigma(\mathbf{k}) + \Sigma_\sigma^{12}(\mathbf{k},\omega)\ , \\ \Delta_\sigma(\mathbf{k}) = \frac{1}{NQ}\sum_{\mathbf{q}} J(\mathbf{k}-\mathbf{q})\langle X_{-\mathbf{q}}^{0\bar\sigma} X_{\mathbf{q}}^{0\sigma}\rangle\ . \qquad (35)$$

The self-energy is calculated in SCBA (24) as in the Hubbard model:

$$\Sigma_{\sigma}^{11(12)}(\mathbf{k},\omega) = \frac{1}{N}\sum_{q} g^2(\mathbf{q},\mathbf{k}-\mathbf{q}) \int\limits_{-\infty}^{+\infty} \frac{dz d\Omega}{\omega - z - \Omega} \times$$

$$\times \frac{1}{2}\left(\tanh\frac{z}{2T} + \coth\frac{\Omega}{2T}\right) A_{\sigma}^{11(12)}(\mathbf{q},z) \times$$

$$\times [-\frac{1}{\pi}\,\mathrm{Im}\, D^{\pm}(\mathbf{k}-\mathbf{q},\Omega + i\delta)]\,, \qquad (36)$$

where the interaction $g(\mathbf{q},\mathbf{k}-\mathbf{q}) = t(\mathbf{q}) - J(\mathbf{k}-\mathbf{q})/2$ and the spectral densities are defined by the corresponding GF:

$$A_{\sigma}^{11(12)}(\mathbf{q},z) = -\frac{1}{\pi}\,\mathrm{Im}\, G_{\sigma}^{11(12)}(\mathbf{q},z+i\delta). \qquad (37)$$

The electron-electron interaction is caused by the spin-charge fluctuations defined by the boson-like commutator GF: $D^{\pm}(\mathbf{q},\Omega) = \langle\langle \mathbf{S}(\mathbf{q})|\mathbf{S}(-\mathbf{q})\rangle\rangle_{\Omega} \pm$ $\pm \langle\langle n(\mathbf{q})|n(-\mathbf{q})\rangle\rangle_{\Omega}/4$ where, in comparison with the Hubbard model, the charge (number) fluctuation contribution is written here explicitly.

The equation for the self-energy (36) is similar to (25) obtained for the Hubbard model if we disregard in the latter the small contribution from the second subband $\propto F_{\sigma}^{11}(\mathbf{k},\omega_1)$. However, contrary to the gap equation (26) in the WCA for the Hubbard model, for the t–J model in the Eq. (35) the frequency-dependent self-energy contribution $\Sigma_{\sigma}^{12}(\mathbf{k},\omega)$ (36) is taken into account. Moreover, in Ref. 81 for the t–J model a full self-consistent solution for the normal GF $G_{\sigma}^{11}(\mathbf{k},\omega)$ in (34) and the corresponding self-energy $\Sigma_{\sigma}^{11}(\mathbf{k},\omega)$ (36) was performed. These calculations for a low hole concentration, $\delta \sim 0.1$, and for a modest AFM correlation length, $\xi \sim 3$, reveal the quasiparticle-like peaks only in the vicinity of the Fermi level (Fig. 3,*a*) and an anomalous behavior for the self-energy $\mathrm{Im}\,\Sigma_{\sigma}^{11}(\mathbf{k},\omega + i\delta) \propto \omega$ close to the Fermi level. The occupation numbers $N(\mathbf{k}) = (1/Q)\langle X_{\mathbf{k}}^{\sigma\sigma}\rangle$ show only a small drop at the Fermi level which is generic for strongly correlated systems (Fig. 3,*b*).

The superconducting T_c was calculated from a linearized gap equation which was solved by direct diagonalization in $(\mathbf{k},\omega)$-space:

$$\Phi_{\sigma}(\mathbf{k},i\omega_n) =$$

$$= \frac{T}{N}\sum_{\mathbf{q}}\sum_{m}\{J(\mathbf{k}-\mathbf{q}) + \lambda_{12}(\mathbf{q},\mathbf{k}-\mathbf{q}|i\omega_n - i\omega_m)\} \times$$

$$\times G_{\sigma}^{11}(\mathbf{q},i\omega_m) G_{\bar{\sigma}}^{11}(\mathbf{q},-i\omega_m)\Phi_{\sigma}(\mathbf{q},i\omega_m)\,, \qquad (38)$$

where the interaction function $\lambda_{12}(\mathbf{q},\mathbf{k}-\mathbf{q}|i\omega_{\nu}) =$ $= g^2(\mathbf{q},\mathbf{k}-\mathbf{q})D^{-}(\mathbf{k}-\mathbf{q},i\omega_{\nu})$ and the Matsubara frequencies $\omega_n = \pi T(2n+1)$ were introduced. Also the eigenfunctions $\Phi_{\sigma}(\mathbf{k},i\omega_n)$ of the Eq. (38) were determined which unambiguously demonstrated the d-wave character of superconducting pairing (for details see [81]).

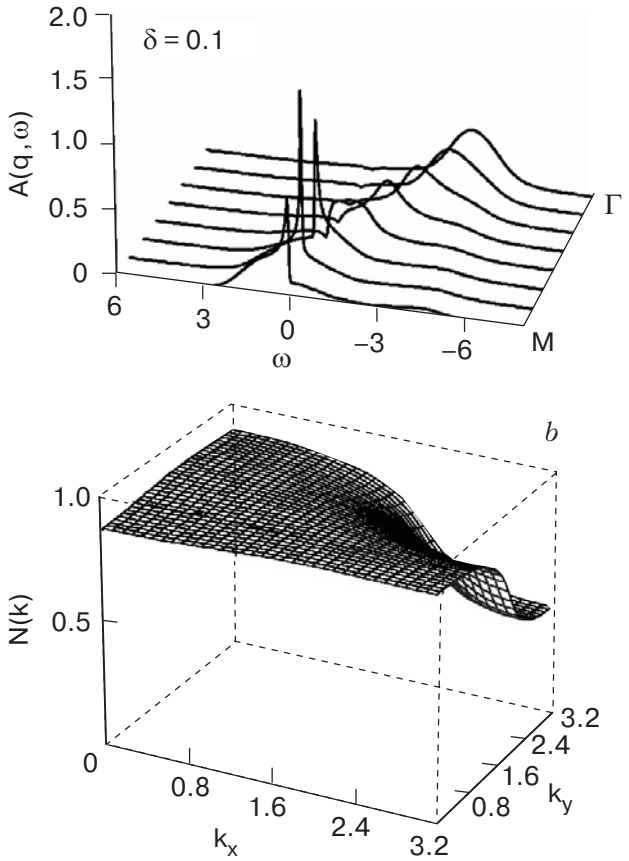

Fig. 3. Spectral density $A_{\sigma}^{11}(\mathbf{q},\omega)$ (37) along the symmetry direction $\mathrm{M}(\pi,\pi) \to \Gamma(00)$ (*a*) and occupation numbers $N(\mathbf{k}) = (1-n/2)^{-1}\langle X_{\mathbf{k}}^{\sigma 0} X_{\mathbf{k}}^{0\sigma}\rangle$ (*b*) at hole concentration $\delta = 0.1$. Energy is measured in units of t with $J = 0.4\,t$ [81].

Comparison of the $T_c(\delta)$ dependence for the Hubbard model in Fig. 2,*a* with the results obtained in [81] for the t–J model, reveals a strong reduction of $T_c^{\max}$ in the latter model due to accounting for a large contribution from the $\mathrm{Im}\,\Sigma_{\sigma}^{11}(\mathbf{k},\omega)$. At the same time, large value of the $\delta_{\mathrm{opt}} \simeq 0.33$ in the t–J model in comparison with experimentally observed $\delta_{\mathrm{opt}} \simeq 0.16$ and $\delta_{\mathrm{opt}} \simeq 0.12$ in the Hubbard model shows that the t–J model cannot properly reproduce the doping dependence of T_c since in the model the weight transfer between the Hubbard subbands under doping is neglected. Therefore, to obtain a reliable values of $T_c(\delta)$ a full self-consistent numerical solution of the Dyson equation in the Hubbard model should be performed.

4. Conclusion

Various theoretical approaches considered in this paper, both of a phenomenological character with a fitted electron–spin-fluctuation interaction as in (1),

and the microscopic theory based on the Hubbard model (3) in the weak correlation limit, as well in the strong correlation limit described by the t–J model (4), unambiguously, demonstrate a possibility of the spin-fluctuation d-wave pairing with high T_c. The clearest description of the magnetic pairing mechanism was obtained within the effective p–d Hubbard model considered in Sec. 2. We have demonstrated that there are essentially *two channels* of superconducting pairing. The first one is the AFM exchange pairing caused by the lowering of the QP kinetic energy produced by the inter-subband hopping in a lattice with a short-range AFM order. The retardation effects in this pairing are negligible, which results in coupling of all charge carriers in the conduction subband. The second one is the conventional spin-fluctuation pairing due to hopping in one Hubbard subband, which is usually considered in the phenomenological approach. We have proved the singlet $d_{x^2-y^2}$-wave superconducting pairing both for the original two-band p–d Hubbard model [89] and for the reduced effective one-band t–J model [81]. It is essential to stress that the both pairing channels are induced by the kinematic interaction, characteristic to the Hubbard model. These mechanisms of superconducting pairing are absent in the fermionic models (for a discussion, see Anderson [27]) and are generic for cuprates revealing strong Coulomb correlations. Therefore, we believe that the proposed superconducting pairing is the relevant mechanism of the high-temperature superconductivity in the copper-oxide materials.

However, to develop a quantitative theory of superconducting pairing in the cuprates one has to take into account a pseudogap formation in the underdoped region of the $T-\delta$ phase diagram. As it was first pointed out by Kampf and Schrieffer [14], the AFM spin fluctuations lead to a pseudogap in the electronic spectrum. A more accurate consideration of the self-energy in the t–J model, in comparison with our results (36), also revealed a pseudogap formation and an effective truncation of the large Fermi surface at low doping caused by short-range AFM fluctuations [106]. By incorporating these results and developing a theory of spin fluctuations in strongly correlated systems within the effective p–d Hubbard model (9), one can hope to develop a self-consistent microscopic pairing theory in the superconducting cuprates.

1. J.G. Bednorz and K.A. Müller, *Z. Phys.* **B64**, 189 (1986).
2. J. Zaanen, G.A. Sawatzky, and J.W. Allen, *Phys. Rev. Lett.* **55**, 418 (1985).
3. P. Bourges, in: *The Gap Symmetry and Fluctuations in High-Temperature Superconductors*, J. Bok, G. Deutscher, D. Pavuna, and S.A. Wolf (eds.), p. 349, Plenum Press, New York (1998); *arXiv:cond-mat/*9901333.
4. A.A. Kordyuk, S.V. Borisenko, A. Koitzsch, J. Fink, M. Knupfer, B. Büchner, H. Berger, G. Margaritondo, C.T. Lin, B. Keimer, S. Ono, and A. Ando, *Phys. Rev. Lett.* **92**, 257006 (2004); A.A. Kordyuk, S.V. Borisenko, V.B. Zabolotnyy, J. Geck, M. Knupfer, J. Fink, B. Büchner, C.T. Lin, B. Keimer, H. Berger, S. Komiya, and A. Ando, *arXiv:cond-mat/*0510760 (2005).
5. P.W. Anderson, *Science* **235**, 1196 (1987); P.W. Anderson, *The Theory of Superconductivity in the High-T_c Cuprates*, Princeton University Press, Princeton (1997).
6. N.M. Plakida, In: *Lectures on the Physics of Highly Correlated Electron Systems, Y*.F. Mancini (ed.), AIP Conference Proceedings, vol. 580, New York (2001), p. 121.
7. M. Cyrot, *Solid State Commun.* **60**, 253 (1986).
8. K. Miyake, S. Schmitt-Rink, and C.P. Varma, *Phys. Rev.* **B34**, 6554 (1986).
9. D.J. Scalapino, E. Loh, Jr., and J.E. Hirsch, *Phys. Rev.* **B34**, 8190 (1986).
10. N.E. Bickers, D.J. Scalapino, and R.T. Scalettar, *Int. J. Mod. Phys.* **B1**, 687 (1987).
11. D.J. Scalapino, *Phys. Rep.* **250**, 329 (1995); *arXiv:cond-mat/*9908287.
12. N. Bulut, *Adv. Physics* **51**, 1587 (2002).
13. J.R. Schrieffer, X.-G. Wen, and S.-C. Zhang, *Phys. Rev. Lett.* **60**, 944 (1989).
14. A.P. Kampf and J.R. Scrieffer, *Phys. Rev.* **B41**, 6399 (1990); *ibid*. **42**, 7967 (1990).
15. J.R. Schrieffer, *Physica* **C185–189**, 17 (1991).
16. D. Pines, *Physica* **B163**, 78 (1990).
17. D. Pines, *Physica* **C235–240**, 113 (1994).
18. A. Millis, H. Monien, and D. Pines, *Phys. Rev.* **B42**, 167 (1990).
19. P. Monthoux, A.V. Balatsky, and D. Pines, *Phys. Rev.* **B46**, 14803 (1992).
20. P. Monthoux and D. Pines, *Phys. Rev.* **B47**, 6069 (1993); *ibid*. **49**, 4261 (1994).
21. P. Monthoux, *Phys. Rev.* **B55**, 15261 (1997).
22. T. Moria, Y. Takahashi, and K. Ueda, *J. Phys. Soc. Jpn.* **59**, 2905 (1990).
23. S. Nakamura, T. Moria, and K. Ueda, *J. Phys. Soc. Jpn.* **65**, 4026 (1996).
24. T. Dahm, J. Erdmenger, K. Scharnberg, and C.T. Rieck, *Phys. Rev.* **B48**, 3896 (1993).
25. M.T. Béal-Monod and K. Maki, *Phys. Rev.* **B53**, 5775 (1996).
26. J.R. Schrieffer, *J. Low Temp. Phys.* **99**, 397 (1995).
27. P.W. Anderson, *Adv. Physics* **46**, 3 (1997).
28. J. Hubbard, *Proc. Roy. Soc. A (London)* **276**, 238 (1963); *ibid*. **277**, 237 (1963).
29. Th. Pruschke, M. Jarrell, and J.K. Freericks, *Adv. Phys.* **44**, 187 (1995).
30. A. Georges, G. Kotliar, W. Krauth, and M. Rozenberg, *Rev. Mod. Phys.* **68**, 13 (1996).

31. Th. Maier, M. Jarrel, Th. Pruschke, and M. H. Hettler, *Rev. Mod. Phys.* **77**, 1027 (2005).
32. Th. Maier, M. Jarrel, Th. Pruschke, and J. Keller, *Phys. Rev. Lett.* **85**, 1524 (2000).
33. Th.A. Maier, M. Jarrell, A. Macridin, and C. Slezak, *Phys. Rev. Lett.* **92**, 027005 (2004).
34. Pao Chien-Hua and N.E. Bickers, *Phys. Rev. Lett.* **72**, 1870 (1994); *Phys. Rev.* **B51**, 16310 (1995).
35. P. Monthoux and D.J. Scalapino, *Phys. Rev. Lett.* **72**, 1874 (1994).
36. S.T. Lenck, J.P. Carbotte, and R.C. Dynes, *Phys. Rev.* **B50**, 10149 (1994).
37. T. Dahm and L. Tewordt, *Phys. Rev. Lett.* **74**, 793 (1995); *Phys. Rev.* **B52**, 1297 (1995).
38. N.E. Bickers, D.J. Scalapino, and S.R. White, *Phys. Rev. Lett.* **62**, 961 (1989).
39. T. Takimoto and Y. Moria, *J. Phys. Soc. Jpn.* **66**, 2459 (1997).
40. D. Manske, I. Eremin, and K.H. Bennemann, *Phys. Rev.* **B62**, 13922 (2000).
41. I.E. Dzyaloshinskii, *Sov. Phys. JETP* **66**, 848 (1987); I.E. Dzyaloshinskii and V.M. Yakovenko, *Sov. Phys. JETP* **67**, 844 (1988).
42. C. Honerkamp and M. Salmhofer, *Phys. Rev. Lett.* **87**, 187004 (2001); *Phys. Rev.* **B64**, 184516 (2001).
43. V. Yu. Irkhin, A. A. Katanin, and M. I. Katsnelson, *Phys. Rev.* **B64**, 165107 (2001).
44. C. Honerkamp, M. Salmhofer, N. Furukawa, and T.M. Rice, *Phys. Rev.* **B63**, 035109 (2001).
45. E. Dagotto, *Rev. Mod. Phys.* **66**, 763 (1994).
46. J. Jaklč and P. Prelovšek, *Adv. Physics* **49**, 1 (2000).
47. D.J. Scalapino, *J. Low Temp. Phys.* **117**, 179 (1999); D.J. Scalapino and S.R. White, *arXiv:cond-mat/*0007515.
48. Shiwei Zhang, J. Carlson, and J.E. Gubernatis, *Phys. Rev. Lett.* **78**, 4486 (1997).
49. C.T. Shih, Y.C. Chen, H.Q. Lin, and T.K. Lee, *Phys. Rev. Lett.* **81**, 1294 (1998).
50. S. Sorella, G.B. Martins, F. Becca, C. Gazza, L. Capriotti, A. Parola, and E. Dagotto, *Phys. Rev. Lett.* **88**, 117002 (2002).
51. Z.B. Huang, H.Q. Lin, and J.E. Gubernatis, *Phys. Rev.* **B64**, 205101 (2001).
52. A.E. Ruckenstein, P.J. Hischfeld, and J. Appel, *Phys. Rev.* **B36**, 857 (1987).
53. Y. Suzumura, Y. Hasegawa, H. and Fukuyama, *J. Phys. Soc. Jpn.* **57**, 401 (1988).
54. Sh. Feng, Z.B. Su, and Yu. Lu, *Phys. Rev.* **B49**, 2368 (1994).
55. N.M. Plakida, *Cond. Matter Phys. (Ukraine)* **5**, 707 (2002); *arXiv:cond-mat/*0210385.
56. G. Kotliar and J. Liu, *Phys. Rev. Lett.* **61**, 1784 (1988).
57. A.E. Ruckenstein and S. Schmitt-Rink, *Phys. Rev.* **B38**, 7188 (1988).
58. M. Grilli and G. Kotliar, *Phys. Rev. Lett.* **64**, 1170 (1990).
59. A. Greco and R. Zeyher, *Eur. Phys. Lett.* **35**, 115 (1996)
60. R. Zeyher and A. Greco, *Z. Phys.* **B104**, 737 (1997).
61. S. Schmitt-Rink, C.M. Varma, and A.E. Ruckenstein, *Phys. Rev. Lett.* **60**, 2793 (1988).
62. C.L. Kane, P.A. Lee, and N. Read, *Phys. Rev.* **B39**, 6880 (1989).
63. G. Martínez and P. Horsch, *Phys. Rev.* **B44**, 317 (1991).
64. Z. Liu and E. Manousakis, *Phys. Rev.* **B45**, 2425 (1992).
65. A. Scherman and M. Schrieber, *Phys. Rev.* **B48**, 7492 (1993); *ibid.* **50**, 12887 (1994).
66. N.M. Plakida, V.S. Oudovenko, and V.Yu. Yushankhai, *Phys. Rev.* **B50**, 6431 (1994).
67. A.F. Barabanov, L.A. Maksimov, and A.V. Mikheenkov, in: *Lectures on the Physics of Highly Correlated Electron Systems, IY*, F. Mancini (ed.), AIP Conference Proceedings, vol. 527, New York (2000), p. 1.
68. E. Dagotto, A. Nazarenko, and A. Moreo, *Phys. Rev. Lett.* **74**, 310 (1995).
69. V.I. Belinicher, A.L. Chernyshov, A.V. Dotsenko, and O.P. Sushkov, *Phys. Rev.* **B51**, 6076 (1995).
70. N.M. Plakida, V.S. Oudovenko, P. Horsch, and A.I. Liechtenstein, *Phys. Rev.* **B55**, R11997 (1997).
71. A. Scherman and M. Schrieber, *Phys. Rev.* **B52**, 10621 (1995).
72. C. Zhang, C. Gros, T.M. Rice, and H. Shiba, *Supercond. Sci. Technol.* **1**, 36 (1988).
73. P.W. Anderson, P.A. Lee, M. Randeria, T.M. Rice, N. Trivedi, and F.C. Zhang, *J. Phys.: Condens. Matter* **16**, R755 (2004).
74. A. Paramekanti, M. Randeria, and N. Trivedi, *Phys. Rev.* **B70**, 054504 (2004).
75. J. Hubbard, *Proc. Roy. Soc. A (London)* **285**, 542 (1965).
76. R.O. Zaitsev and V.A. Ivanov, *Sov. Phys. Solid State* **29**, 2554 (1987); *ibid.* **29**, 3111 (1987); *Int. J. Mod. Phys.* **B5**, 153 (1988); *Physica* **C153–155**, 1295 (1988).
77. Yu.A. Izyumov and Yu.N. Scryabin, *Statistical Mechanics of Magnetically Ordered Systems*, Consultant Bureau, New York (1989).
78. Yu.A. Izyumov and B.M. Letfulov, *J. Phys.: Condens. Matter* **3**, 5373 (1991).
79. Yu.A. Izyumov and B.M. Letfulov, *Intern. J. Modern Phys.* **B6**, 321 (1992).
80. N.M. Plakida, V.Yu. Yushankhai, and I.V. Stasyuk, *Physica* **C160**, 80 (1989); V.Yu. Yushankhai, N.M. Plakida, and P. Kalinay, *Physica* **C174**, 401 (1991).
81. N.M. Plakida and V.S. Oudovenko, *Phys. Rev.* **B59**, 11949 (1999).
82. D.N. Zubarev, *Usp. Fiz. Nauk* **71**, 71 (1960) [*Sov. Phys. Usp.* **3**, 320 (1960)].
83. N.M. Plakida, *Phys. Lett.* **A43**, 481 (1973).
84. N.M. Plakida and I.V. Stasyuk, *Modern Phys. Lett.* **2**, 969 (1988).
85. N.N. Bogoliubov, V.L. Aksenov, and N.M. Plakida, *Physica* **C153–155**, 99 (1988).
86. N.M. Plakida, *JETP Lett.* **74**, 36 (2001).
87. N.M. Plakida, R. Hayn, and J.-L. Richard, *Phys. Rev.* **B51**, 16599 (1995).

88. N.M. Plakida, *Physica* **C282–287**, 1737 (1997).
89. N.M. Plakida, L. Anton, S. Adam, and Gh. Adam, *Zh. Exp. Theor. Fiz.* **124**, 367 (2003) [*JETP* **97**, 331 (2003)].
90. J. Beenen and D.M. Edwards, *Phys. Rev.* **B52**, 13636 (1995).
91. A. Avella, F. Mancini, D. Villani, and H. Matsumoto, *Physica* **C282–287**, 1757 (1997); F. Mancini, H. Matsumoto, and V.S. Oudovenko, *Physica* **B230–232**, 915 (1997).
92. T.D. Stanescu, I. Martin, and Ph. Phillips, *Phys. Rev.* **B62**, 4300 (2000).
93. W.E. Pickett, *Rev. Mod. Phys.* **61**, 433 (1989).
94. O.K. Andersen, A.I. Liechtenstein, O. Jepsen, and F. Paulsen, *J. Phys. Chem. Solids*, **56**, 1573 (1997).
95. V.I. Anisimov, F. Aryasetiawan, and A.I. Lichtenstein, *J. Phys.: Condens. Matter* **9**, 767 (1997).
96. V.J. Emery, *Phys. Rev. Lett.* **58**, 2794 (1987).
97. C.M. Varma, S. Schmitt-Rink, and E. Abrahams, *Solid State Commun.* **62**, 681 (1987).
98. Yu.B. Gaididei and V.M. Loktev, *Phys. Status Solidi* **147**, 307 (1988).
99. V.M. Loktev, *Fiz. Nizk. Temp.* **31**, 645 (2005) [*Low Temp. Phys.* **31**, 490 (2005)].
100. S.V. Maleev (unpublished)
101. F.C. Zhang and T.M. Rice, *Phys. Rev.* **B37**, 3759 (1988).
102. V.Yu. Yushankhai, V.S. Oudovenko, and R. Hayn, *Phys. Rev.* **B55**, 15562 (1997).
103. L.F. Feiner, J.H. Jefferson, and R. Raimondi, *Phys. Rev.* **B53**, 8751 (1996).
104. K.A. Lokshin, D.A. Pavlov, S.N. Putilin, et al., *Phys. Rev.* **B63**, 064511 (2001).
105. G.-M. Zhao, K.K. Singh, and D.E. Morris, *Phys. Rev.* **B50**, 4112 (1994).
106. P. Prelovšek and A. Ramšak, *Phys. Rev.* **B65**, 174529 (2002).